Journal of Signal Processing, Vol. 13, No. 6, pp. 477-485, November 2009

PAPER

Central Pattern Generator Network with High Controllability for Tripod Gait Generator and Its Application

Tatsuji Tokiwa and Takeshi Yamakawa

Graduate School of Life Science and Systems Engineering, Kyushu Institute of Technology
2-4 Hibikino, Wakamatsu-ku, Kitakyushu, Fukuoka 808-0196, Japan
E-mail: tokiwa@brain.kyutech.ac.jp

Abstract **We have proposed a central pattern generator (CPG) network for quadrupedal locomotion signal generators. The proposed network comprised four CPGs and one rhythm generator and had the feature of independent controllability of the amplitude and period. In this study, the proposed network is applied to generate a tripod gait typical of hexapod insects. The network retains the feature of independent controllability and can be logically designed. In order to verify the effectiveness of the proposed method, first the operations of the network are simulated. Moreover, a hexapod robot named Yamac-H is designed and the CPG network is implemented in it. Through experimental results, we confirm that the designed robot generates the tripod gait and can walk on flat ground. The network is suitable for a locomotion signal generator used to generate a tripod gait, because its configuration and the values of connection weights can be logically and uniquely designed, and the amplitude and period of the output signals can be independently controlled.**

Keywords: central pattern generator, van der Pol equation, hexapod locomotion signal generator, tripod gait, hexapod robot

1. Introduction

It is well known that locomotion signals such as walking, running, swimming and flying are generated and controlled by the central nervous system so called the central pattern generator (CPG) [1]. A CPG is a neuromethodological circuit found in both invertebrate and vertebrate animals that can generate locomotion signals without requiring sensory information. The locomotion signals can be classified into periodic patterns known as gaits. For example, hexapod insects such as stick insects typically exhibit two types of gait called tripod and tetrapod gaits.

In recent years, many CPG network models [1]-[3] have been reported. See also [4] for a review of previous research on CPG networks. CPG network models comprise a number of oscillators that are described by higher-order differential equations. In this paper, the oscillators are called CPGs. In conventional network models, CPGs are coupled to each other through connection weights because the structures of the CPG network are designed from the viewpoint of physiology.

One of our target applications is a legged robot. CPGs are assigned at each leg, which is controlled by an output signal from each CPG. The output signals of the CPGs are controlled by adjusting some of the connection weights through trial and error and by changing the configuration of the CPG network. Generally, walking speed can be controlled by changing the amplitudes of signals. Additionally, if it is necessary to increase the speed, the periods of the signals must be controlled. However, it is not so easy to control and analyze the output signals of the CPG network in terms of the amplitude and period of each CPG and the phase difference between CPGs. This is because some of the CPGs in the network are described by higher-order differential equations with mutual connections between the CPGs. There are many CPG networks that can control a hexapod robot and generate the tripod gait [5]-[12]. However, almost all these CPG networks were designed on the basis of biological concepts. Therefore, considerable time is required to determine appropriate connection weights and the configuration of the network. And, the amplitudes and periods of the output signals can not be estimated beforehand.

To solve these problems, we have proposed a CPG network with a feature of high designability and controllability [13]-[15]. The network was designed from the viewpoint of not physiology but engineering. When designing a locomotion signal generator, each CPG must satisfy two necessary and sufficient conditions: it must have (1) a limit cycle, which is represented by higher-order nonlinear differential equations, and (2) high controllability of the amplitude and period of the signal in the stable state, i.e., in the limit cycle. Moreover, in the CPG network, the phase differences between the CPGs must be controlled. Our network comprises a rhythm generator (RG) and some CPGs. Each CPG and the RG are described by the Van der Pol (VDP) equation. We consider that this equation is suitable for the CPG model, because the VDP equation is the simplest model that has a limit cycle and features independent controllability of the amplitude and period of the limit cycle [16]. The amplitude and period of the output signal from each CPG and the RG are controlled almost independently by external signals, because the CPGs and RG are designed such that the feature of the VDP equation is maintained. In order to control the phase shift between CPGs, the period of the output signal from each CPG is temporarily controlled through connections that are only conjunctions between the RG and each CPG. The configuration of the CPG network can be logically and uniquely determined on the basis of a gait transition. In our previous study, the proposed CPG network was applied to a quadrupedal locomotion signal generator to generate typical quadrupedal locomotion signals, which are the walk, trot, bound, and gallop modes.

Generally speaking, it is not easy to extend conventional CPG networks to produce other locomotion signal generators for other numbers of legs. This is because the analysis becomes complicated when a large number of nonlinear oscillators are generated, and the output signals from CPGs cannot be predicted. In this respect, our proposed CPG network has the potential to be extended to produce multilegged locomotion signal generators regardless of the number of legs, because the proposed network has the feature of independent controllability and because the phase differences are always shifted according to the difference between the output signals of two oscillators. In other words, the amplitude, period, and phase difference can be controlled independently of the number of CPGs in the proposed CPG network. As an example, a CPG network for hexapod locomotion is designed by applying the same concept as that used in our previous study. In this paper, first the procedure of CPG network configuration is described, and it is confirmed that the proposed CPG network retains the features of independent controllability and designability of our previous network. Moreover, in order to verify the effectiveness of the proposed method, a hexapod robot named Yamac-H is produced, on which some experiments are conducted.

2. Tripod Gait

It is well known that stick insects produce different gaits under various conditions. Methods of generating the gaits have been extensively studied using stick insects and cockroaches [17] [18]. The tripod gait is one of the most typical gaits in hexapod insects. Fig. 1 shows the step pattern of the tripod gait [19]. LF, LM, LH, RF, RM, and RH stand for left foreleg, left middle-leg, left hind-leg, right foreleg, right middle-leg, and right hind-leg, respec-

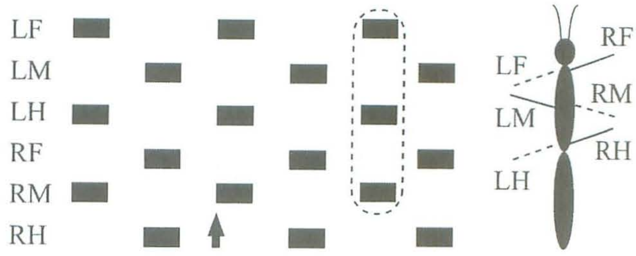

Fig. 1 Step pattern of tripod gait [19]

tively. Each swing phase is represented by a black bar, and the space between bars represents the stance phase. The timescale reads from left to right. The picture on the right schematically shows the position of the legs of the insect at the time indicated by the arrow. In the picture, dashed legs denote legs that are in the swing phase. Such a record facilitates the quantification of the following features, which are used to characterize a gait. (1) Period: the duration of a step. The stance and swing phases are measured from the swing phase onset. (2) Lag: the time interval between the beginning of a swing phase in one leg and the beginning of a swing phase in another. (3) Phase: the lag between two legs divided by the period of the first leg. The phase makes the value for lag independent of the period duration. In the tripod gait, the ipsilateral fore- and hind legs and the contralateral middle leg are swung forward simultaneously. For example, LM, RF, and RH are in the stance phase and LF, LH, and RM are in the swing phase as shown by the dotted circle in Fig. 1. In this gait, it is typical that both legs of one segment have a relative phase of 0.5, which means that they are exactly alternating. The tripot gait is used throughout the insect's whole range of walking speeds and is maintained even when the animal is changing direction [17]. Stick insects can change their walking speed by adjusting the period of the output signals. On the other hand, turns are produced by changes in step length rather than step period [19]. In order to design a CPG network with these features, it is necessary to design a network where the amplitude and period of the output signals can be independently controlled.

3. CPG Network Model

The CPG network comprises several CPGs and one RG and is designed on the basis of the VDP equation.

3.1 CPG model

The CPG model is derived from the VDP equation [20] and is represented by Eq. (1). The VDP equation is the simplest model that has a limit cycle and the feature of independent controllability of both the amplitude and period of the limit cycle. Therefore, we consider that the VDP equation is suitable for the CPG model. The ith CPG model (CPG_i) is written as Eq. (1).

$$\frac{d^2x_i}{dt^2} - 2\epsilon\left(A^2 - x_i^2\right)\frac{dx_i}{dt} + B_i^2 x_i = 0 \tag{1}$$

Here the parameter ϵ is a small constant called the nonlinearity coefficient. The value of x_i is the output signal of CPG_i (i= 1, 2,$\cdots$, n), where n denotes the required number of CPGs in the CPG network. The amplitude and period of x_i in the stable state can be controlled by parameters A and B_i, respectively. Oscillatory solutions are always obtained from the VDP equation when $A<B_i$. In particular, it was confirmed that the period is inversely proportional to B_i and that the amplitude reaches $2A$ in the stable state [16] [15] [21].

In order to control the phase difference between CPGs, the phase of each CPG must be temporally shifted. The parameter B_i represented in the following equation is utilized to control the phase of CPG_i.

$$B_i = B_{nf} + b_i \tag{2}$$

$$b_i = k(x_i - X_i) \tag{3}$$

Here X_i, B_{nf}, and k denote the target signal, the natural frequency of the CPGs, and the gain factor, respectively. The target signal is an oscillation that has the desired phase difference and is assigned by network designer beforehand. The method of assignment is discussed in Sect. 3.2. The value of b_i determines the phase shift of CPG_i. After the phase difference between the output signal x_i and target signal X_i becomes 0, the value of b_i approaches 0. The value of k can be used to control the time taken to attain the stable state.

The block diagram of CPG_i is shown in Fig. 2. The period of the output signal x_i is controlled by b_i so that the phase difference between the control and target signals becomes 0.

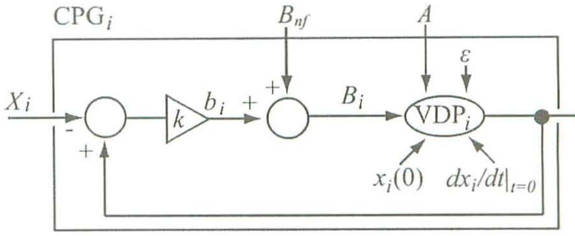

Fig. 2 Block diagram of CPG_i

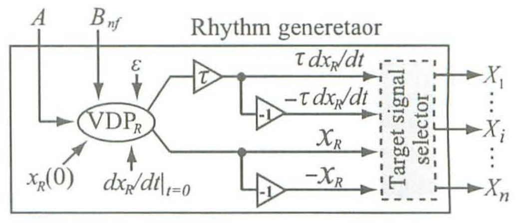

Fig. 3 Block diagram of RG

3.2 Rhythm generator

The configuration of the RG is shown in Fig. 3. The RG is designed as the target signal generator on the basis of the VDP equation.

$$\frac{d^2x_R}{dt^2} - 2\epsilon\left(A^2 - x_R^2\right)\frac{dx_R}{dt} + B_{nf}^2 x_R = 0 \tag{4}$$

The value of x_R or $\frac{dx_R}{dt}$ is used as the target signals. Target signal X_i is represented by Eq. (5). c_{i1} and c_{i2} are connection weights with a value of -1, 0, or 1, and are determined by the gait transition we intend to control. Either c_{i1} or c_{i2} is always 0.

$$X_i = c_{i1}x_R + c_{i2}\tau\frac{dx_R}{dt} \tag{5}$$

τ determines the dimensions of x_R and $\frac{dx_R}{dt}$, and adjusts the amplitude of $\frac{dx_R}{dt}$ to ensure that the amplitudes of x_R and $\frac{dx_R}{dt}$ remain constant even if the parameters A and B_{nf} are changed. τ is defined as in Eq. (6).

$$\tau = \frac{\max(x_R)}{\max(\frac{dx_R}{dt})} = \frac{2A}{\max(\frac{dx_R}{dt})} \tag{6}$$

Here $max(\cdot)$ is the max function. Since the amplitude of x_R is controlled by parameter A, the value of $\max(x_R)$ can be rewritten as $2A$. On the other hand, the value of $\max(\frac{dx_R}{dt})$ is taken from simulation results, because it cannot be estimated beforehand. The values of A and B_{nf} in the RG are equal to those in the CPG in Fig. 2. The desired target signals of the CPGs are selected by the target signal selector in Fig. 3. The function of the selector is expressed as Eq. (5). For instance, when $-x_R$ is selected for target signal X_i, the combination of c_{i1} and c_{i2} is set to be $c_{i1}=-1$ and $c_{i2}=0$.

3.3 CPG network design for the tripod gait

Fig. 4 shows the gait transition of the tripod gait. The arrows represent the directions of the phase transition. The output signals of CPG_1, CPG_2, CPG_3, CPG_4, CPG_5, and CPG_6 are sent to the LF, RF, LM, RM, LH, and RH, respectively. The procedure for designing the CPG network for the typical hexapod gait is as follows.

1. One RG and 6 CPGs are prepared. The number of CPGs corresponds to the number of legs.
2. Parameters A and B_{nf} are input to the RG and CPGs. Because of this structure, each CPG can achieve independent controllability of the amplitude and period of the output signal x_i.
3. The output signal of each CPG is allocated as the control signal to each leg.
4. The target signal X_i of CPG_i is determined on the basis of the gait transitions. In this study, target signal

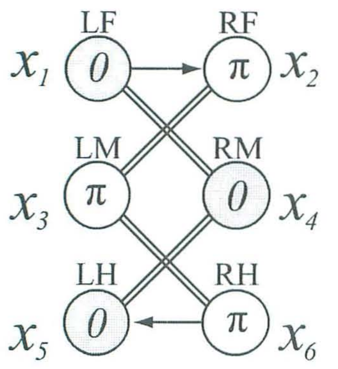

Fig. 4 Gait transition of tripod gait

X_i is designed on the basis of the gait transition of the tripod gait (Fig. 4).

5. x_R is selected for consistency target signal X_1. The output signal of CPG_1 acts as the reference signal for calculating the phase differences between CPG_1 and the other CPGs (c_{11}=1, c_{12}=0).
6. The output signal x_2 controls RF. Since the phase difference between LF and RF is π, $-x_R$ is selected for target signal X_2 (c_{21}=−1, c_{22}=0).
7. $-x_R$ is selected for target signal X_3, because the phase difference between LF and LM is π (c_{31}=−1, c_{32}=0).
8. x_R is selected for target signal X_4, because the phase difference between LF and RM is 0 (c_{41}=1, c_{42}=0).
9. x_R is selected for target signal X_5, because the phase difference between LF and LH is 0 (c_{51}=1, c_{52}=0).
10. The output signal x_6 controls RH. Since the phase difference between LF and RH is π, $-x_R$ is selected for target signal X_6 (c_{61}=−1, c_{62}=0).

The configuration of the CPG network is shown in Fig. 5 [22]. From this design procedure, we confirm that the connection weights c_{i1} and c_{i2} and the configuration of the CPG network can be logically and uniquely determined from the gait transition.

3.4 Flexible mode

In our previous research, the proposed CPG network generates only four phase differences: 0, $\frac{\pi}{2}$, π, and $\frac{3\pi}{2}$. However, it can be easily imagined that a variety of phase differences can be freely generated if a constant value is temporarily assigned to b_i. It is considered that this feature can be regarded as a flexible mode. The operation can be represented by Eq. (7).

$$b_i = \begin{cases} b_i(t) & , if\ in\ flexible\ mode \\ k\,(x_i - X_i) & , otherwise\ (normal\ mode) \end{cases} \quad (7)$$

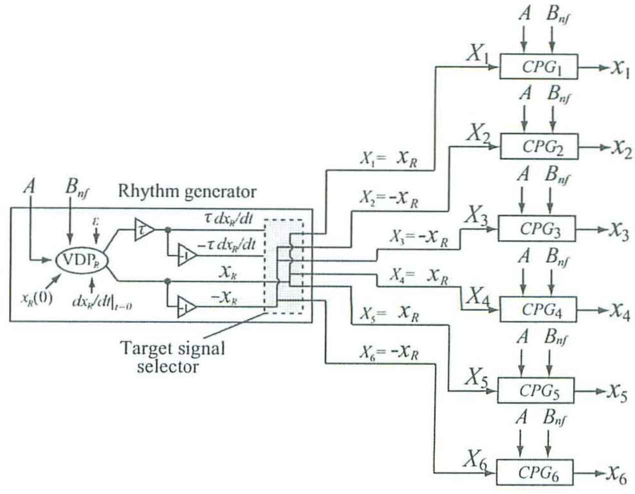

Fig. 5 CPG network configuration for tripod gait

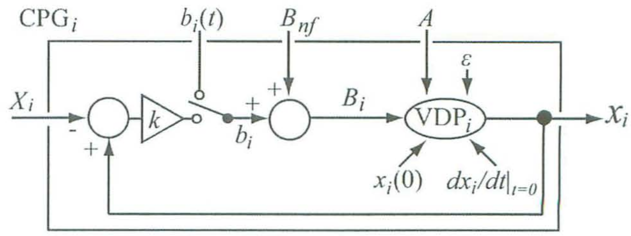

Fig. 6 Block diagram of CPG_i with flexibility

Fig. 6 shows a block diagram of CPG_i with flexibility. X_i, x_i, k, $b_i(t)$, ϵ, $x_i(0)$, and $\frac{dx_i}{dt}|_{t=0}$ denote the target signal, the output signal of CPG_i, the gain factor, an external signal, the nonlinearity coefficient, and the initial values of x_i and $\frac{dx_i}{dt}$, respectively. According to the situation, either normal mode or flexible mode is applied, in other words, either $b_i(t)$ or $k\,(x_i - X_i)$ is chosen for b_i. In normal mode, the period of the output signal x_i is controlled by adjusting b_i until $(x_i - X_i)$ becomes 0 as mentioned above. On the other hand, in flexible mode, the period of x_i is controlled until $(x_i - X_i)$ becomes $b_i\,(t)$.

A stability analysis of the flexible mode can be conducted by using the VDP equation. This is because a constant value is assigned as $b_i\,(t)$ during the mode. In other words, $B_{nf} + b_i\,(t)$ can be considered as a constant value. Therefore, it is confirmed that the CPG network with the flexible mode has a limit cycle.

4. Hexapod Robot Yamac-H

In order to implement the CPG network, a hexapod robot called Yamac-H is designed in this paper. The design procedure was as follows. Autodesk Inventor was used for designing Yamac-H. Each part of the robot was made of acrylonitrile-butadiene-styrene (ABS) resin shaped into the desired size using an NC cutting machine. Table 1 shows the physical parameters of Yamac-H, which is 210 [mm] in length, 120 [mm] in width, 130 [mm] in height,

Table 1 Physical parameters of Yamac-H

mass of the robot	564 g
width of the body	120 mm
width of the robot	200 mm
length of the body	205 mm
height of the robot	130 mm
length of the robot	210 mm
length of 1st legs	65 mm
length of 2nd legs	60 mm

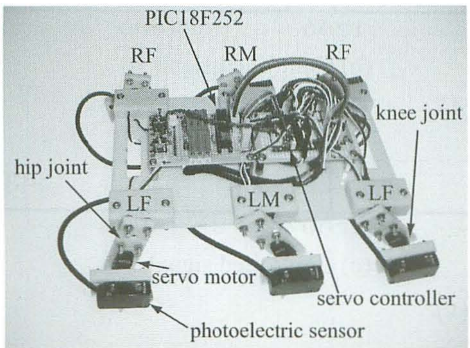

Fig. 7 Appearance of Yamac-H

Table 2 List of Yamac-H components

Name	Model name	no.
Servo motor	Futaba S3110	12
Servo controller	AGB65-RSC	1
PIC	PIC18F252	1
Sensor	Keyence PZ-V11	6

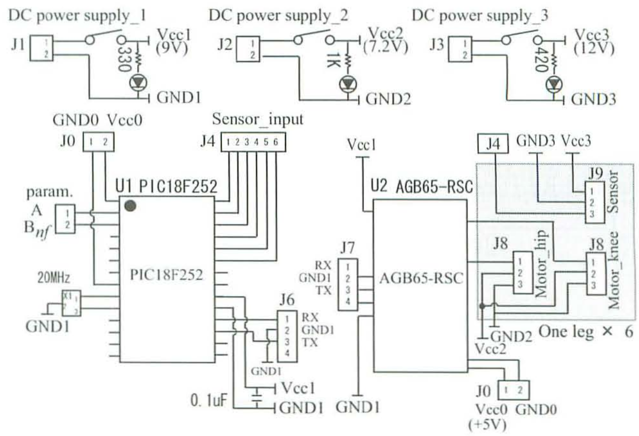

Fig. 8 Control circuit of Yamac-H

and 564 [g] in weight, and has 6 legs. Each leg has two joints, namely, the hip and knee joints, which rotate around the pitch axis. Fig. 7 shows the appearence of Yamac-H. A DC motor is attached on each joint. A photoelectric sensor that can detect the time when the tip of the leg collides with the ground is attached on the knee joint. The main components of Yamac-H are listed in Table 2. The proposed CPG network is calculated using a peripheral interface controller (PIC) with product number PIC18F252. Each hip joint is controlled by the output signal x_i from the CPGs and each knee joint is operated in accordance with the movement of the hip joint in each leg. The peripheral circuit of Yamac-H is shown in Fig. 8. The power supplies for controlling the motor controller, servo motors, and sensors have voltages of 9 [V], 7.2 [V], and 12 [V], respectively.

5. Simulation and Experimental Results

5.1 Simulation results for CPG network

In order to verify the effectiveness of the proposed method, operations of the CPG network were investigated by the 4th-order Runge-Kutta method. Figs. 9(a) and 9(b) show the simulation results for the tripod gait. In this simulation, ϵ, dt, and k were 0.2, 0.1, and 1, respectively. As has been mentioned, for the hexapedal locomotion generator, c_{11}, c_{21}, c_{31}, c_{41}, c_{51}, c_{61}, c_{12}, c_{22}, c_{32}, c_{42}, c_{52}, and c_{62} were determined to be 1, -1, -1, 1, 1, -1, 0, 0, 0, 0, 0, and 0, respectively. Parameters A and B_{nf} were provided by external signals and were 0.5 and 1, respectively. Ultimately, these parameters A and B_{nf} are determined in view of a desired walking speed of robots, a rotation angle of legs, and a length of each leg. The initial values of x_i and $\frac{dx_i}{dt}$ were chosen randomly. In this simulation, the following values were selected: x_R=0.4, x_1=0.1, x_2=−0.3, x_3=0.4, x_4=−0.1, x_5=−0.4, x_6=0.7, $\frac{dx_R}{dt}$=0.5, $\frac{dx_1}{dt}$=0.2, $\frac{dx_2}{dt}$=0.3, $\frac{dx_3}{dt}$=−0.3, $\frac{dx_4}{dt}$=−0.2, $\frac{dx_5}{dt}$=0.3, and $\frac{dx_6}{dt}$=−0.1. The output values of the CPGs and the transitions of b_i were measured for up to 800 steps. In Fig. 9(a), it is confirmed that the amplitude of the output signals becomes almost $2A$ in a stable state and that the phase differences between CPGs are controlled, as shown in Fig. 4. From Fig. 9(b), it is found that b_i becomes 0 after the phase of each x_i is controlled by adjusting target signal X_i. In this simulation, the operation that the value of b_i omits 0.3 or less was added, because X_i is not necessarily equal to x_i. This process is applied in all other experiments. The horizontal line in Fig. 9(b) indicates that b_i=0.3.

Fig. 10 shows the simulation result for the output signal in normal and flexible modes. In the Figure, the transitions of four output signals from the CPGs and the controlled signals of b_2, b_3, and b_4 are shown. In this simulation, the CPG network comprised one RG and four CPGs. Up to 1200 steps, normal mode was selected and the phase differences of the four output signals were controlled to 0. After that, flexible mode was selected and b_2, b_3, and b_4 were set to 0.2 by external signals. The application time for each b_i was as follows: b_2 from 1200 steps to 1250 steps, b_3 from 1200 steps to 1300 steps, and b_4 from 1200

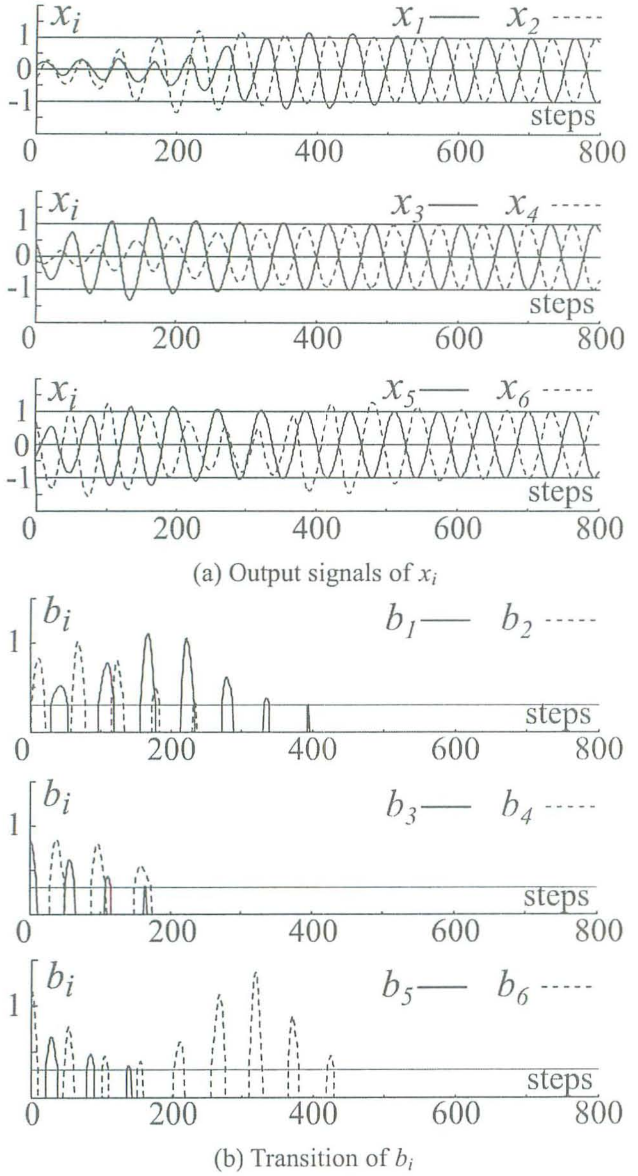

(a) Output signals of x_i

(b) Transition of b_i

Fig. 9 Simulation results for tripod gait

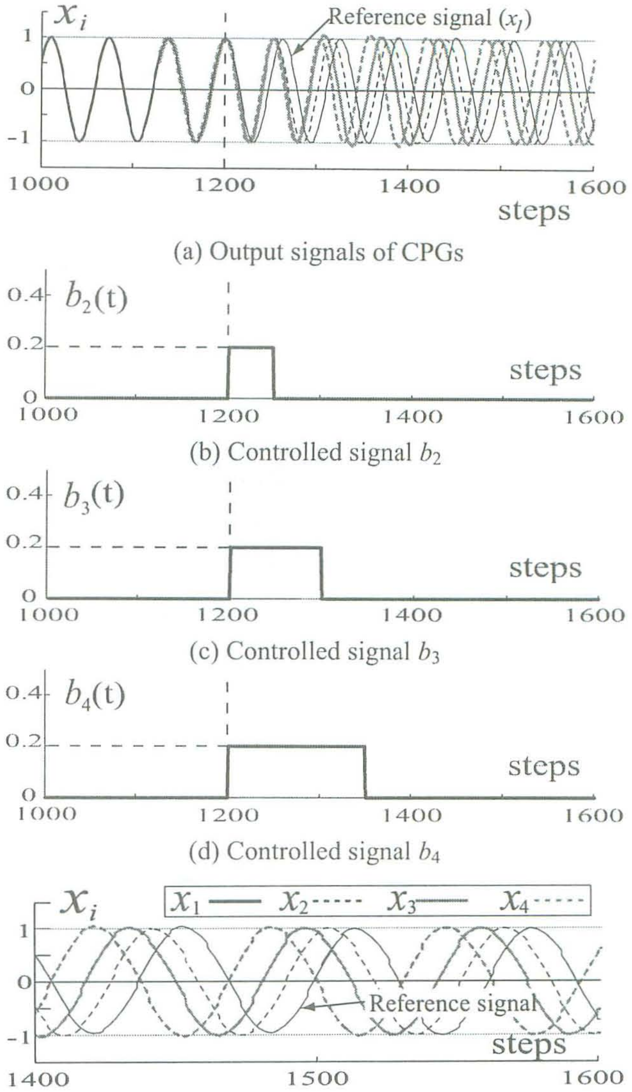

(a) Output signals of CPGs

(b) Controlled signal b_2

(c) Controlled signal b_3

(d) Controlled signal b_4

(e) Output signals of CPGs

Fig. 10 Simulation results for CPG network in normal and flexible modes

steps to 1350 steps. Even after 1200 steps, b_1 was always set to 0 so that the output signal x_1 was a reference signal with respect to other output signals x_2, x_3, and x_4. From the simulation result, it was confirmed that the controlled values of these phase differences were proportional to the time for which the external signals were applied. In this study, $b_i(t)$ was assigned by a designer beforehand. However, ultimately, $b_i(t)$ can be generated by robots. For instance, it is assumed that a circuit that can calculate the total current consumption of all servo motors is installed and that the generation of a gait with low power consumption is required. When the current consumption suddenly increases owing to environmental changes, the walking gait must be slightly changed. In this situation, $b_i(t)$ can be utilized. A value of $b_i(t)$ proportional to the current consumption can be automatically determined, which can be assigned until the consumption decreases.

5.2 Experimental results for Yamac-H

Fig. 11 shows the walking behaviors of Yamac-H. The tripod gait has two phases termed phase P_1 and phase P_2. The arrows in Figs. 11(b) and 11(d) indicate the legs on the ground. In phase P_1, RF, LM, and RH are in the stance phase and RM, LF, and LH are in the swing phase. Reversely, in phase P_2, RF, LM, and RH are in the swing phase and RM, LF, and LH are in the stance phase. These photographs indicate that Yamac-H can walk on flat terrain and that the tripod gait can be generated using the output signals shown in Fig. 9(a).

In the case when $A = 0.5$ and $B_{nf} = 1.0$ used in Sec. 5.1, Yamac-H walked dynamically with a stride of approx-

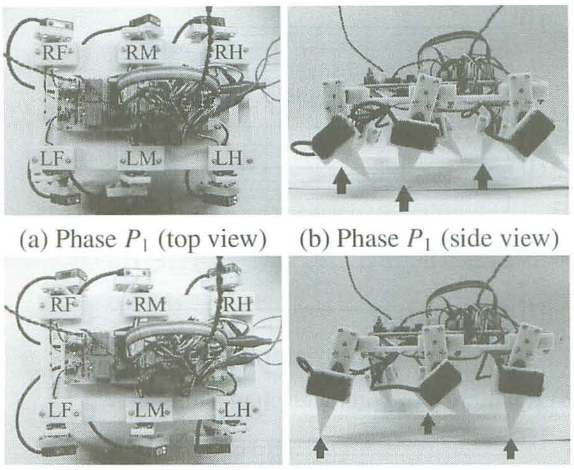

(a) Phase P_1 (top view) (b) Phase P_1 (side view)

(c) Phase P_2 (top view) (d) Phase P_2 (side view)

Fig. 11 Walking behaviors of Yamac-H

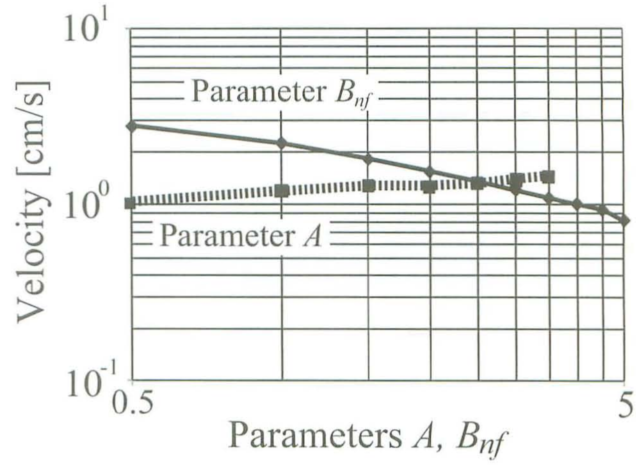

Fig. 12 Walking velocity of Yamac-H for different values of parameters A and B_{nf}

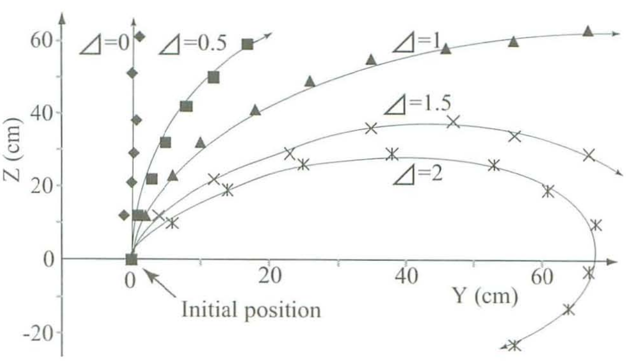

Fig. 13 Walking trajectories of Yamac-H

imately 30 [mm], a period of 1.7 [s], and a speed of 2.2 [cm/s]. Moreover, the walking speed was measured for various values of A and B_{nf}. Fig. 12 shows the experimental results. It is confirmed that the parameter B_{nf} can greatly change the velocity. On the other hand, the speed varies less with parameter A. In this study, the values of A and B_{nf} were assigned by a designer beforehand. In order to clear the effects of these parameters, only the output signals from CPGs in a stable state were used for controlling each hip joint. In the experiments, ϵ, dt, and k were 0.2, 0.1, and 1, respectively. As has been mentioned, c_{11}, c_{21}, c_{31}, c_{41}, c_{51}, c_{61}, c_{12}, c_{22}, c_{32}, c_{42}, c_{52}, and c_{62} were set as 1, -1, -1, 1, 1, -1, 0, 0, 0, 0, 0, and 0, respectively, and the initial values of x_i and $\frac{dx_i}{dt}$ were chosen randomly. These values were calculated using the PIC. When the relationship between the speed and parameter A was measured, B_{nf} was set as 4, and when the relationship between the speed and parameter B_{nf} was measured, A was set as 0.5.

Fig. 13 shows walking trajectories of Yamac-H. The five trajectories were measured while changing the amplitude of the output signals through parameter A. Positions of Yamac-H were plotted with respect to every ten seconds. In this experiment, the parameter B_{nf} was set as 2.5. The right side (RF, RM, RH) and left side (LF, LM, LH) amplitudes were separately controlled in this experiment only. Δ denotes the difference of parameter A between the one of CPG_1, CPG_3, CPG_5 and the one of CPG_2, CPG_4, CPG_6. From Fig. 13, it is confirmed that the larger the value of Δ, the more bent the walking trajectory becomes. As mentioned in Sect. 2, turns are produced by changes in the amplitude, that is, the step length. These changes of walking direction can be easily achieved by the parameter A, because the proposed CPG network has the high controllability of the output signal x_i.

6. Discussion

A key concept of the proposed CPG network is as follows. Typical quadrupedal and tripod gaits can be described using only four different phases: 0, $\frac{\pi}{2}$, π, and $\frac{3\pi}{2}$. Therefore, in the proposed CPG network, the control signal produced by the RG for each CPG can be represented by $\pm x$ and $\pm\frac{dx}{dt}$, which are the calculation results obtained from the VDP equation.

In the proposed CPG network, the amplitude and period of the output signals were simulated for different values of parameters A and B_{nf}. Fig. 14 shows the simulation results. In this simulation, ϵ and the initial values of x_R, x_i, $\frac{dx_R}{dt}$, and $\frac{dx_i}{dt}$ were randomly assigned (i= 1, 2,$\cdots$, 6). In the case of A=0, the CPG network operated as a damped oscillation. Oscillatory solutions were always obtained from the network when $A<B_{nf}$. In Figs. 14(b) and 14(c), each dotted line represents the theoretical line discussed in Sect. 3.1. From the simulation results, it was confirmed that the amplitude and period of the limit cycle could be independently controlled by varying parameters A and B_{nf}, respectively. In particular, in a steady state, the amplitude becomes almost $2A$, and the period is inversely proportional to B_{nf}. These experimental results show that the proposed

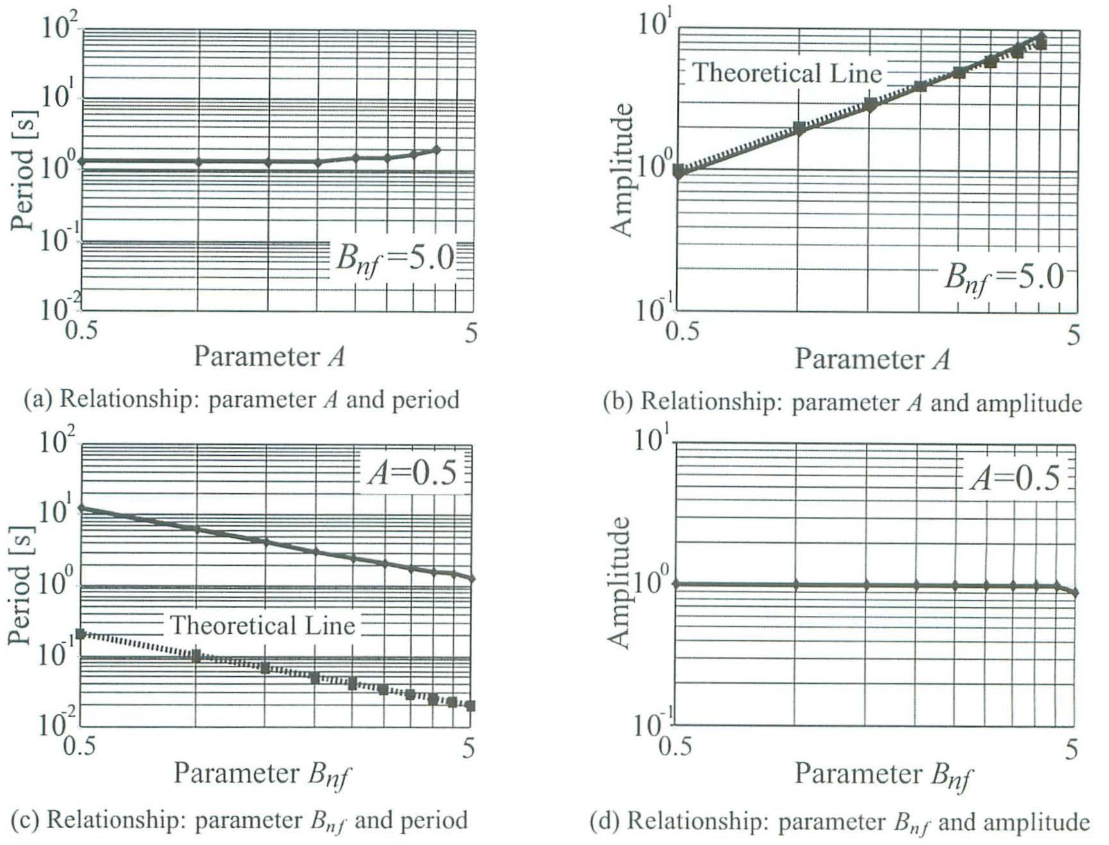

Fig. 14 Output signals for different values of the two parameters

CPG network maintains the feature of independent controllability of our previous CPG network. This feature is expected to be useful for locomotion signal generators for hexapod robots, because it means that robot designers can logically adjust the walking speed through parameters A and B_{nf}.

In this paper, we did not show the effectiveness of the flexible mode using Yamac-H. The mode will be required in situations such as a change in external environment and a breakdown of the legs or body. In order to validate the model using an actual robot, it is necessary to install other types of sensors that can detect these changes and to alter the configuration of Yamac-H. In our experiments, in order to demonstrate that the proposed CPG model can be applied to a real robot, the walking behaviors of Yamac-H in the tripod gait were analyzed for various values of the parameters. Analysis of the behavior of Yamac-H in the flexible mode is planned as further work.

7. Conclusions

We have proposed a CPG network with high controllability for generating a tripod gait. The network is suitable for a locomotion generator model for hexapod robots, because its configuration and connection weights can be logically and uniquely designed and because the amplitude of the output signals can be easily estimated by the designer beforehand. The output signals from the CPG network were implemented in a motor controller to control a hexapod robot named Yamac-H. From our experimental results, it was confirmed that Yamac-H generated the tripod gait, was able to walk on flat ground, and was able to change the walking directions. The behaviors can be easily accomplished by changing the only one parameter in each CPG, because the proposed CPG network has the feature of high controllability in comparison with the conventional ones. Moreover, the network can generate output signals with a variety of phase differences using external signals. Some gaits which were composed by those output signals will be able to adapt to changes of external environment. We emphasize that the proposed CPG network is suitable for a hexapod locomotion signal generator.

Acknowledgments

This work was supported in part by a Grant-in-Aid for Specially Promoted Research (Project No. 20001008), "Identification of Epileptogenic Focus by Employing Soft Computing and Establishment of Minimally Invasive and Definitive Surgery" (Project Director: T. Yamakawa) granted in 2008 to Graduate School of Life Science and Systems Engineering, Kyushu Institute of Technology; Graduate School of Medicine, Yamaguchi University; and Faculty of Engineering, Shizuoka University by the Ministry of Education, Culture, Sports, Science and Technology, Japan.

References

[1] F. Delcomyn: Neural basis of rhythmic behavior in animals, Science, Vol. 210, pp. 492-498, 1980.

[2] T. G. Brown: The intrinsic factors in the act of progression in the mammal, Proc. R. Soc. London, Ser. B, Vol. 84, pp. 308-319, 1911.

[3] K. Matsuoka: Sustained oscillations generated by mutually inhibiting neurons with adaptation, Biol. Cybern., Vol. 52, pp. 367-376, 1983.

[4] A. J. Ijspeert: Central pattern generetaors for locomotion control in animals and robots: A review, Neural Networks, Vol. 21, pp. 642-653, 2008.

[5] F. Delcomyn: Walking robots and the central and peripheral control of locomotion in insects, Autonomous Robots, Vol. 7, pp. 259-270, 1999.

[6] R. D. Beer, et al.: A distributed neural network architecture for hexapod robot locomotion, Neural Computation, Vol. 4, pp. 356-365, 1992.

[7] H. Cruse, et al.: Walking: A complex behavior controlled by simple networks, Adaptive Behavior, Vol. 3, No. 4, pp. 385-418, 1995.

[8] D. Graham: Simulation of a model for the coordination of leg movement in free walking insects, Biol. Cybern., Vol. 26, pp. 187-198, 1977.

[9] S. Kimura, M. Yano and H. Shimizu: A self-organizing model of walking patterns of insects, Biol. Cybern., Vol. 69, pp. 183-193, 1993.

[10] H. Cruse: A new model describing the coordination patterns of the legs of a walking stick insect, Biol. Cybern, Vol. 32, pp. 107-113, 1979.

[11] H. Cruse: A quantitative model of the walking incorporating central and peripheral influences. I. The control of the individual leg, Biol. Cybern, Vol. 37, pp. 131-136, 1980.

[12] H. Cruse: A quantitative model of the walking inforporating central and peripheral influences. II. The connections between the different legs, Biol. Cybern, Vol. 37, pp. 137-144, 1980.

[13] T. Tokiwa and T. Yamakawa: Central pattern generator network model with independent controllability, Journal of Signal Processing, Vol. 12, No. 6, pp. 441-448, 2008.

[14] T. Yamakawa and T. Tokiwa: Control system, oscillation controller and a method generating controlled signals, Japanese patent (in Japanese), Application No. TOKUGAN 2008-52752, March 4, 2008.

[15] T. Tokiwa and T. Yamakawa: Central pattern generator network model with independent controllability, RISP International Workshop on Nonlinear Circuits and Signal Processing (NCSP'08), pp. 156-159, 2008.

[16] T. Tokiwa and T. Yamakawa: Modified van der Pol oscillators for hardware design, RISP International Workshop on Nonlinear Circuits and Signal Processing (NCSP'07), pp. 595-598, 2007.

[17] D. Graham: An analysis of walking in the first instar and adult stick insect (Carausius morosus), J. Comp. Physiol., Vol. 81, pp. 23-52, 1972.

[18] G. M. Hughes: The co-ordination of insect movements. I. The walking movements of insects, Journal of Experimental Biology, Vol. 29, pp. 267-285, 1952.

[19] U. Bässler: Neural Basis of Elementary Behavior in Stick Insects, Springer-Verlag Berlin Heidelberg New York, 1983.

[20] van der Pol: On relaxation oscillations, Phil. Mag., No. 2, pp. 987-993, 1926.

[21] L. A. Pipes and L. R. Harvill: Applied Mathematics for Engineers and Physicists, McGraw-Hill Education, Third Edition, 1970.

[22] T. Tokiwa, M. G. Paulin and T. Yamakawa: A construction of a mathematical model expressing an alternating tripod gait -An application for a 3D stick insect behavior model-, The 20st Robotics and Mechatronics Conference 2008 (ROBOMEC 2008), pp. 1A1-E01(1)-(4), 2008.

Tokiwa Tatsuji received his B. Eng., M. Eng., and Ph. D. degrees from Kyushu Institute of Technology, Japan in 2004, 2006, and 2009 respectively. He is currently a postdoctoral fellow in the Kyushu Institute of Technology. His research interests include signal prosessing, central pattern generator and robotics. He is a member of the Journal of Signal Processing, the Robotics Society of Japan, IEEE Systems, Man, and Cybernetics Society, and IEEE Robotics and Automation Society.

Takeshi Yamakawa received his B. Eng. degree in Electronics Engineering in 1969 from Kyushu Institute of Technology, Tobata, and his M. Eng. degree in Electronics Engineering in 1971 from Tohoku University, both in Japan. He received his Ph.D. degree for his studies of electrochemical devices in 1974 from Tohoku University, Japan.

He was a former Associate Professor at Kumamoto University. He joined the faculty of Computer Science and Systems Engineering, Kyushu Institute of Technology (KIT), Iizuka, Japan as a full professor in April, 1989. He established a national foundation, the Fuzzy Logic Systems Institute (FLSI), in Japan in 1990. He is currently the vice chairman of FLSI and also a professor of the Faculty of Life Science and Systems Engineering of KIT, Wakamatsu, Kitakyushu, Japan.

His main research interest is in hardware implementation of fuzzy systems, fuzzy neural networks, chaotic systems and self-organizing systems as well as micro-devices for biochemical analysis. He holds 11 patents in the U.S.A., 4 patents in Europe, 1 patent in Australia and 1 patent in Taiwan; he has also applied for more than 90 patents in Japan. He received fifteen awards such as the International MOISIL Prize and the Gold Medal in 1994.

Dr. Yamakawa is a fellow of the International Fuzzy Systems Association (IFSA) and Japan Society of Fuzzy Theory and Intelligent Informatics (SOFT), and a senior member of IEEE. He is a member of the editorial board and a regional editor of 10 international professional journals. He contributed to more than 80 international conferences as an organizer or a member of the organizing/programming committee. He has served and is currently serving as the chairman of various academic societies and institutes.

(Received May 15, 2009; revised August 17, 2009)